6th Croatian Conference on Geometry and Graphics
Baška, 6–10 September 2026

ABSTRACTS

EDITORS:
Tomislav Došlić, Ema Jurkin

PUBLISHER:
Croatian Society for Geometry and Graphics

Donor:
SAND d.o.o.

Patronage:
International Society for Geometry and Graphics

Supported by the Ministry of Science, Education and Youth of the Republic of Croatia and the Foundation of Croatian Academy of Sciences and Arts.

Contents

Plenary lectures

Minimal and Maximal Surfaces: A Comparative Geometric Perspective

Ljiljana Primorac Gajčić
J. J. Strossmayer University of Osijek, School of Applied Mathematics and Informatics, Osijek, Croatia
e-mail: ljiljana.primorac@mathos.hr

Minimal surfaces in Euclidean space and maximal surfaces in Lorentz–Minkowski space are among the most extensively studied objects in differential geometry. Both classes are characterized by vanishing mean curvature and arise naturally as critical points of variational problems. Despite these similarities, the different metric structures of the ambient spaces lead to substantial differences in their geometric behavior, giving rise to phenomena that are unique to the Lorentzian setting.
This lecture presents a comparative overview of minimal and maximal surfaces with an emphasis on the influence of the causal character of curves on the geometry of the associated surfaces. Special attention is devoted to maximal surfaces associated with null curves, including null scrolls, which provide a rich source of examples in Lorentz–Minkowski geometry.

Key words: minimal surfaces, maximal surfaces, Lorentz–Minkowski space, null scrolls

MSC 2020: 53A10, 53B30, 53A35

References

[1] Filipan, I., Milin Šipuš, Ž., Primorac Gajčić, Lj., Null-Translation Surfaces with Constant Curvatures in Lorentz–Minkowski 3-Space, *Rad Hrvat. Akad. Znan. Umjet. Mat. Znan.* **27**(555) (2023), 219–230.

[2] Filipan, I., Milin Šipuš, Ž., Primorac Gajčić, Lj., Cycloidal maximal surfaces in the 3-dimensional Lorentz-Minkowski space, *Filomat* **40**(1) (2026), 251–268.

[3] López, R., Kaya, S., On the duality between rotational minimal surfaces and maximal surfaces,, *J. Math. Anal. Appl.* **458**(1) (2017), 345–360.

[4] Milin Šipuš, Ž., Primorac Gajčić, Lj., Protrka, I., Null Scrolls with Prescribed Curvatures in Lorentz–Minkowski 3-Space, *An. Șt. Univ. Ovidius Constanța* **28**(3) (2020), 229–240.

[5] Osserman, R., *A Survey of Minimal Surfaces*, Dover Publications, New York, 1986.

Classical Notions and Problems in Thurston Geometries of non-Constant Curvatures

Jenő Szirmai
Budapest University of Technology and Economics, Institute of Mathematics, Budapest, Hungary
e-mail: szirmai@math.bme.hu

One way to understanding the internal structure of geometries is through the elementary notions and theorems of the space under study. Thus, understanding the structure of Thurston geometries i.e. homogeneous, complete, simply connected Riemann ones (see [1]), can also provide important information.

In the study of the internal structures of Thurston spaces, it is worth distinguishing two significantly different directions related to either the translation distance or the geodesic distance. d^g is the usual geodesic distance function, and d^t is the translation distance function. Thus we obtain two types of curves, triangles, bisector surfaces (and two types of the corresponding Dirichlet-Voronoi cells) etc. by the two different distance functions.

In this talk, we will look for those classical concepts and theorems that can be defined or fulfilled in Thurston geometry in some form, related to both distance concepts. This will help us better understand the structure of each geometry and find similarities and differences.

In the presentation we will address the following questions:

1. Concepts and properties of the translation and geodesic triangles (see [6], [1]). In each Thurston space we have already examined the possible internal angle sums of the geodesic and translational triangles and their surfaces.

2. A second important direction is the study of Apollonius surfaces (see [5], [4]) and their special cases the bisector surfaces. These surfaces have an important role in connection to Dirichlet-Voronoi cells. D-V-cells are relevant for tilings, ball packings and coverings and thus for crystallography because it cannot be ruled out that under certain extreme conditions, materials "crystallize" under conditions other than Euclidean ones.

3. The Euclidean Ceva's and Menelaus' theorems (see [4]) are well known, and these can be extended to geometries with constant curvature. Extension to further Thurston geometries is possible by generalizing the concept of simple relation. In these geometries, the extension of the *geometry-dependent simple ratio* plays an important role and indicates its importance. Here the simple ratio can be described by various functions within the considered geometry through its projective embedding.

4. Pappus's hexagon and Desargues's theorem play a very important role in the axiomatic structure of projective geometry. We will examine the role of these theorems in the case of Thurston geometries with non-constant curvature. Here we only mention the **Nil** geometry, in whose projective model the geodesic curves are helix-like and fit onto geodesic **Nil** cylinders of revolution with fibrum axes. We investigate relations for geodesic cylinders and thus also geodesic curves, which lead to a result similar to Pappus' hexagon theorem.

5. Among the classic questions, packings and covering questions cannot be missing, which are also related to material structure problems. Here, in addition to ball packings and coverings, packing and coverings with cylinders (see [7], [6], [3]) are also reviewed.

We only review a few questions here, but these investigations raise many additional problems, the solution of which will provide insight into the structure of Thurton geometries and new knowledge about the relationships between constant curvature geometries and other Thurston geometries.

Key words: Thurston geometries; geodesic curves, translation curves, geodesic and translation triangles; spheres, cylinders; sphere packings and coverings, lattices

MSC 2020: 53A20, 53A35, 52C17, 52C22, 52B15, 57M12, 57M25, 52C35, 53B20

References

[1] Csima, G., Szirmai, J., Translation-like Apollonius and triangular surfaces in non-constant curvature Thurston geometries, *Results Math.* **80**, 190, (2025).

[2] Molnár, E., The projective interpretation of the eight 3-dimensional homogeneous geometries, *Beitr. Algebra Geom.* **38** (2) (1997), 261–288.

[3] Sajtos, J., Szirmai, J., Lattice-like Packings and Coverings with Congruent Translation Balls and Cylinders in **Sol** geometry, *Quaestiones Mathematicae*, (2026), 1–23, `https://doi.org/10.2989/16073606.2026.2649569`

[4] Szirmai, J., Apollonius surfaces, circumscribed spheres of tetrahedra, Menelaus' and Ceva's theorems in $\mathbf{S}^2\times\mathbf{R}$ and $\mathbf{H}^2\times\mathbf{R}$ geometries, *Q. J. Math.* **73** (2022), 477–494.

[5] Szirmai, J., Bisector surfaces and circumscribed spheres of tetrahedra derived by translation curves in **Sol** geometry, *New York J. Math.* **25** (2019), 107–122.

[6] Szirmai, J., Classical Notions and Problems in Thurston Geometries, *International Electronic Journal of Geometry* **16** (2) (2023), 608–643.

[7] Szirmai, J., Fibre-like cylinders, their packings and coverings in $\widetilde{\mathbf{SL_2R}}$ space, *Results Math.* **79**, 123 (2024).

From Roots to Imaging Imaginary

Michal Zamboj
Charles University, Faculty of Education, Prague, Czech Republic
e-mail: michal.zamboj@pedf.cuni.cz

If there is one mathematical story that has been retold countless times, yet never often enough, it is the story of complex numbers. They represent a remarkable abstract extension of mathematical language that has driven innumerable advances across many fields. In this contribution, however, we focus exclusively on the development of their graphical representations.

In searching for the historical roots of these representations, we encounter the tension between the algebraic and geometric languages of the sixteenth century. While algebraic methods introduced new arithmetic rules for solving cubic equations, it was the synthetic geometry of the Greeks that was called upon to support and validate these discoveries. Fundamental steps toward uniting symbolic and visual perspectives were taken through the ingenious ideas of French mathematicians. Of particular importance was the transition introduced by Descartes from a numerical magnitude to a geometric point representing a non-real, or imaginary, root [2]. A second major influence on our subsequent investigation within the framework of incidence projective geometry is the concept of involution, which establishes a correspondence between numbers and points on a line [3]. These initial ideas lead us to a wide range of both well-known and lesser-known representations of complex geometric points and to the relationships between them throughout history.

Special attention is devoted to Poncelet's principle of continuity [5, 7] and to von Staudt's synthetic constructions of algebraic operations in projective geometry [1, 8, 9]. We describe the general principle of constructing products of two-dimensional numbers on models of quadrics in three-dimensional space, such as the Riemann–Neumann sphere [6] and Grünwald's cone [4]. This ultimately leads to a projective classification of two-dimensional number systems according to the incidence relation between a given quadric and a line.

Key words: imaginary elements, complex geometry, geometric visualization, complex numbers, hypercomplex numbers

MSC 2020: 51M15, 14N05, 01A65

References

[1] Coxeter, H. S. M., Beck, G., *The Real Projective Plane*, 3rd ed., Springer-Verlag, New York, 1992.

[2] Descartes, R., *La Géométrie*, Jan Maire, Leiden, 1637.

[3] Desargues, G., *Brouillon project d'une atteinte aux événements des rencontres du cône avec un plan*, Paris, 1639.

[4] Grünwald, J., Über duale Zahlen und ihre Anwendung in der Geometrie, *Monatshefte für Mathematik und Physik* **17** (1906), 81–136.

[5] Hatton, J. L. S., *The Theory of the Imaginary in Geometry: Together with the Trigonometry of the Imaginary*, Cambridge University Press, Cambridge, 1920.

[6] Neumann, C., *Vorlesungen über Riemann's Theorie der Abel'schen Integrale*, B. G. Teubner, Leipzig, 1884.

[7] Poncelet, J. V., *Traité des propriétés projectives des figures*, Bachelier, Paris, 1822.

[8] von Staudt, K. G. C., *Geometrie der Lage*, F. Korn, Nürnberg, 1847.

[9] von Staudt, K. G. C., *Beiträge zur Geometrie der Lage*, 3 vols., F. Korn, Nürnberg, 1856–1860.

Contributed talks

Generative Body Plan of a Ribbed Vault System with Irregular Spatial Loop Morphology for Contemporary Roof Structures

Davor Andrić
University of Zagreb Faculty of Architecture, Zagreb, Croatia
e-mail: dandric@arhitekt.hr

Nataša Jakšić
University of Zagreb Faculty of Architecture, Zagreb, Croatia
e-mail: njaksic@arhitekt.hr

Late Gothic churches are characterized by ribbed, net-vault geometry rather than smooth ceiling surfaces. Such geometries enable the construction of rib systems over diverse floor plans and column arrangements. Some rib systems like that in the Church of Saint Barbara in Kutna Hora designed by Benedikt Ried [2] exhibit spatial loops and circular vault patterns. The rib network, the centers of arches and the underlying floor plan define the unique architectural character of these vaults.

This work, inspired by the Gothic circular vault pattern, which is both geometrically distinctive and resembles natural forms, explores a simple parametric procedure – implemented as Grasshopper definition in Rhino3D, conceived as a generative framework capable of producing contemporary, biomimetic free-form vault structures. The aim is to retain the character of the historical template while introducing controlled geometric variation on smooth surfaces.

Using basic Voronoi-based geometry generation, a range of geometries with different characters can be generated, ranging from crystalline configurations to organic loop structures. This is achieved by using the points in the cell boundaries as control points for interpolation curves and adjusting curve smoothness. The procedure involves projecting points and curves to a reference plane and back to curved surfaces with curve extrusion and surface offset, as well as determining curve-region intersections to find column positions to complement the free-form geometry of the vault. Since the forms are not given in advance, but emerge through dynamic processes of variation, the same generative scheme, or body plan [1], can produce multiple formal actualisations of the desired character and spatial qualities.

Key words: parametric geometry, ribbed vaults, body plan, free-form structures, biomimetic design

References

[1] DeLanda, M., *Intensive Science and Virtual Philosophy*, London, Bloomsbury Academic, 2013.

[2] Fehr, G., *Benedikt Ried: Ein deutscher Baumeister zwischen Gotik und Renaissance in Böhmen*, München, Callwey, 1961.

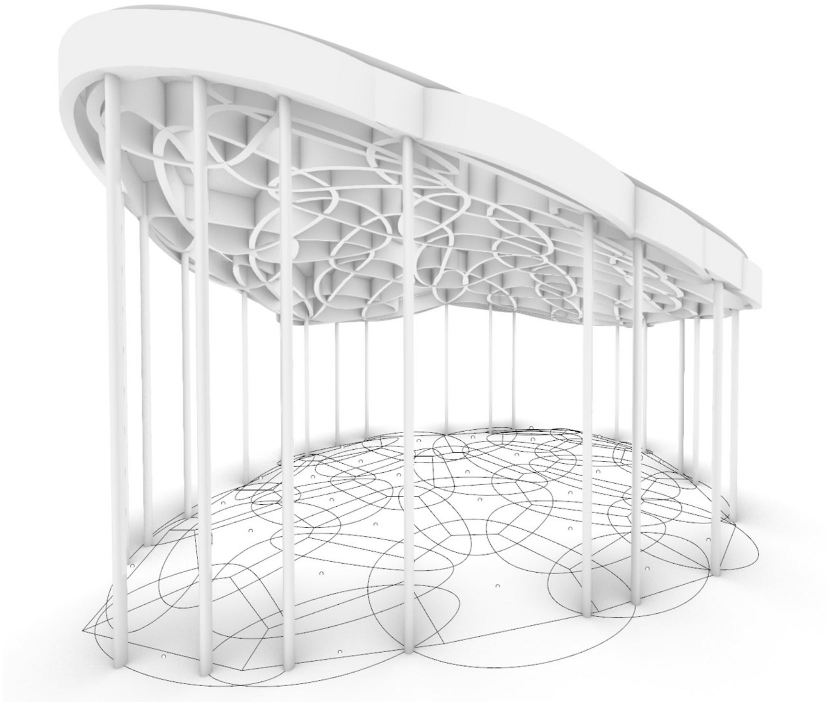

Figure 1: One of many possible instances of the shared body-plan generative procedure for a spatial loop ribbed-vault system. The geometry generation process begins with points and curves on the ground plane and culminates in a three-dimensional roof geometry supported by columns.

Acknowledgments. The Research was conducted as a part of the Tjelesni nacrt nosivih konstrukcija zgrada - corpus structuralium (CorSt) project at the University of Zagreb, Faculty of Architecture, Croatia. The project received EU funding through the Croatian National Recovery and Resilience Plan (NRRP) under the EU 581 Recovery and Resilience Facility (RRF).

Artificial Intelligence and Spatial Cognition

Tamás Balla
Eszterházy Károly Catholic University, Eger, Hungary
e-mail: balla.tamas@uni-eszterhazy.hu

Miklós Hoffmann
Eszterházy Károly Catholic University, Eger, Hungary
e-mail: hoffmann.miklos@uni-eszterhazy.hu

In this lecture, we explore the relationship between artificial intelligence and spatial cognition. At first glance, artificial intelligence appears to have a strong understanding of, for example, perspective and visual scenes—it can generate striking images and seamlessly insert objects into existing images or videos. However, beneath this apparent competence lie significant deficiencies in spatial cognition. The gap between human spatial cognition and the capabilities of artificial intelligence is far greater than the impressive results of generative AI might suggest. The current limitations of AI in spatial cognition are not merely software shortcomings but fundamental representational limitations.

The insertion of objects into existing images or videos is often successful because the background already provides numerous spatial constraints: converging parallel lines, the ground plane, shadow directions, object scale, and local textures are all explicitly available. In such cases, the generative model does not have to solve a complete 3D reconstruction problem from scratch. Instead, it only needs to generate pixels or latent representations that are perceptually consistent with an already highly constrained 2D visual field.

Recent research has shown that although AI-generated images are visually impressive, closer inspection frequently reveals geometric inconsistencies and impossible structures—similar to Escher-like impossible objects—because language-based generative models lack an internal 3D world model.

Key words: spatial cognition, artificial intelligence, mental cutting test

References

[1] Schnabel, T., Tomlinson, K., Swaminathan, A., Neville, J., Lost in transmission: When and why llms fail to reason globally, *Adv. Neural Inf. Process. Syst.* **34** (2026), 138944–138982.

[2] Yang, A., Fu, C., Jia, Q., Dong, W., Ma, M., Chen, H., Yang, F.,Wu, H., Evaluating and enhancing spatial cognition abilities of large language models, *Int. J. Geogr. Inf. Sci.* **39** (2025), 2009–2044.

Exploring the World of Pseudo-Geodesics on the Torus

Christian Clemenz
University of Applied Arts Vienna, Vienna, Austria
e-mail: christian.clemenz@uni-ak.ac.at

Boris Odehnal
University of Applied Arts Vienna, Vienna, Austria
e-mail: boris.odehnal@uni-ak.ac.at

We take an in-depth look at the pseudo-geodesic curves that arise from our numeric construction algorithm when it is applied on the torus. In particular, we focus on curves that seemingly close after a sufficient amount of iterations. We attempt to classify them by finding special characteristics that can identify groups of similar or related curves.

Additionally, we analyze the tangents found on those curves using their Plücker coordinates. Our goal is to determine whether these tangents form a quadratic complex, and therefore, may also be tangent to a quadric. In that context, we also apply our algorithm to the horn and spindle torus as their inversions on the sphere form cylinders and cones respectively. We investigate the properties of the pseudo-geodesics after the inversion in order to find connections to special curves on the cylinder and cone.

Key words: pseudo-geodesic, numeric construction, quadratic complex

MSC 2020: 53-08

References

[1] B. Odehnal, C. Clemenz, A Numerical Approach towards Pseudo-Geodesics, *ICGG 2026 – Proceedings of the 22nd International Conference on Geometry and Graphics* **1** (2026)

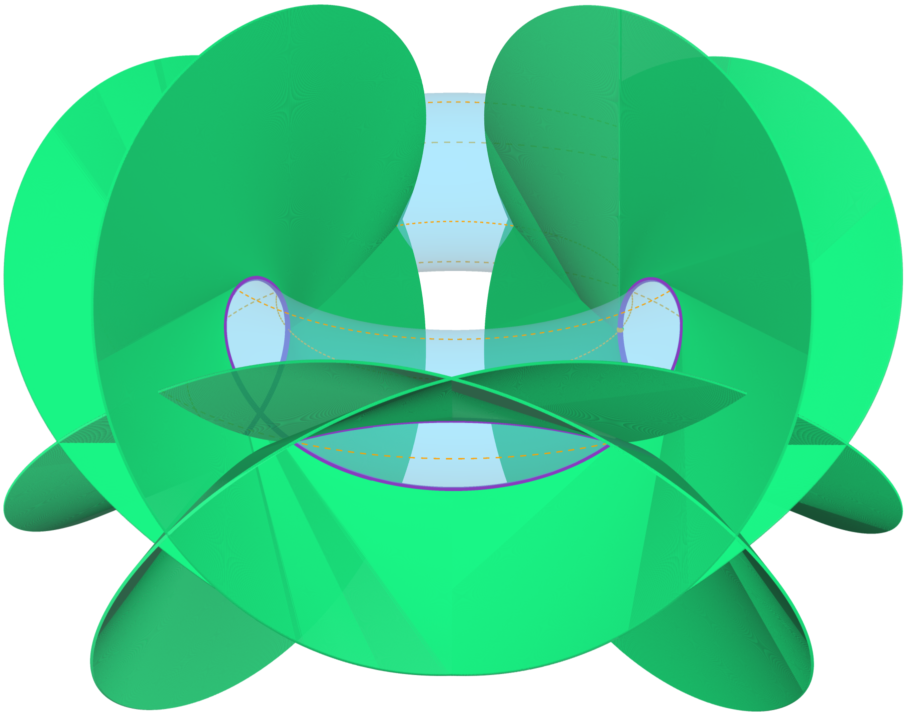

Figure 1: Visualization of the tangents found on a closed pseudo-geodesic on the ring torus.

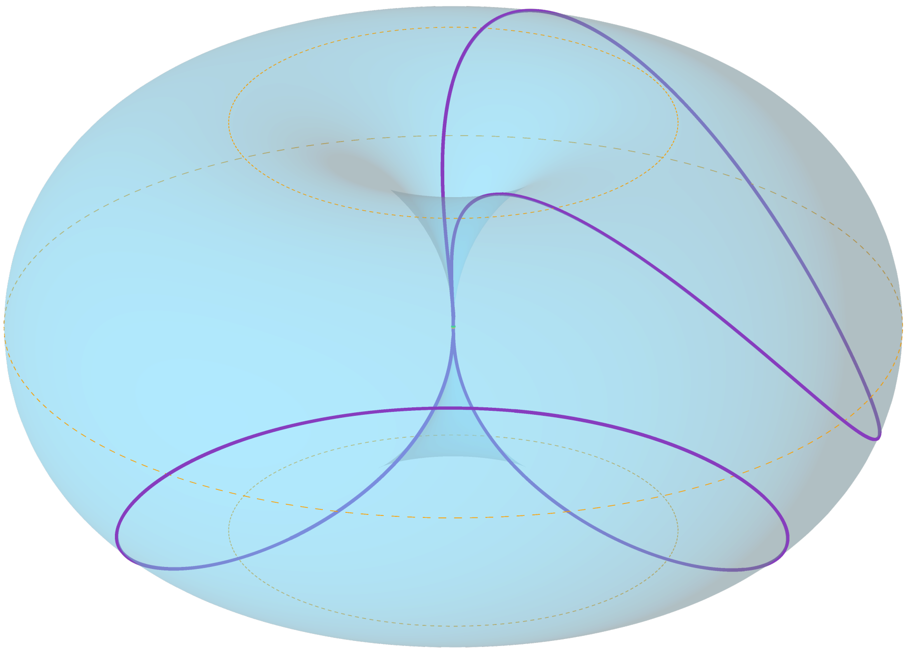

Figure 2: A seemingly closed pseudo-geodesic on the horn torus that passes through the singularity.

Generalized Apollonius Circles as Equioptic Curves of Circles in Constant Curvature Geometries

Géza Csima
University of Debrecen, Faculty of Engineering, Debrecen, Hungary
Budapest University of Technology and Economics, Faculty of Natural Science, Budapest, Hungary
e-mail: csimageza@gmail.com

We extend the old definition of the Apollonius circle in such a way that it results in the same curve in Euclidean geometry but will be more convenient in hyperbolic and spherical geometries. We show that there exists an Apollonius circle of the centers of two circles that coincides with their equioptic curves, as in Euclidean geometry.

Key words: hyperbolic geometry, spherical geometry, Apollonius circle, isoptic curves, equioptic curves

MSC 2020: 51M04, 51M09, 53A35

A Comparison of Two Assessment Approaches for Evaluating Problem-Solving Competencies in Higher Education

Petra Daković
University of Zagreb Faculty of Organization and Informatics, Varaždin, Croatia
e-mail: pdakovic@foi.hr

Blaženka Divjak
University of Zagreb Faculty of Organization and Informatics, Varaždin, Croatia
e-mail: blazenka.divjak@foi.hr

Aim

The main objective of this study is to investigate the relationship between students' performance on problem-solving tasks and their overall performance in the course, as well as to compare the outcomes associated with the two assessment approaches.

Background

The course assessment structure was modified between two consecutive academic years. In the first year, students were assessed through three midterm exams, a project assignment, and continuous assessment activities. The project required students to solve a practical problem by selecting and applying an appropriate mathematical methodology and could be completed over an extended period, potentially in teams.

In the second year, the assessment structure was redesigned. The project component was replaced by continuous problem-solving activities conducted throughout the semester, including problem-based exercises, quizzes, and an oral examination. These activities were intended to assess students' ability to apply mathematical concepts in a more continuous and individual manner.

Planned Analyses

First, a problem-solving performance score will be defined separately for each academic year. In the first year, this score will be based primarily on the project assignment, while in the second year it will be derived from the problem-solving activities implemented throughout the semester, including problem-based exercises and relevant examination components.

Correlation analyses will then be conducted separately for each academic year to examine the association between performance on problem-solving tasks and performance on other course assessments. The goal is to determine whether success in problem-oriented activities is related to success in other forms of assessment and to identify potential differences in these relationships across the two assessment systems.

Finally, the two academic years will be compared with respect to students' achievement in the problem-solving component. This comparison will provide insight into whether students were able to obtain higher levels of achievement through the project-based approach or through the continuous problem-solving assessment approach implemented throughout the semester.

Expected Contribution

The study will contribute to understanding how different assessment designs evaluate and support the development of problem-solving competencies in higher education. In particular, it will provide evidence on whether a project-based assessment or a continuous problem-solving approach is more strongly associated with overall student achievement.

Key words: assessment design, higher education, problem-solving skills, project-based assessment, continuous assessment, student achievement, educational evaluation, correlation analysis, mathematics education, learning outcomes

Directed Sequential Arrangements of Families of Circles

Tomislav Došlić
University of Zagreb Faculty of Civil Engineering, Zagreb, Croatia
e-mail: doslic@grad.hr

Biserka Kolarec
University of Zagreb Faculty of Agriculture, Zagreb, Croatia
e-mail: bkudelic@agr.hr

Marina Ninčević
University of Zagreb Faculty of Agriculture, Zagreb, Croatia
e-mail: mnincevic@agr.hr

We study sequential arrangements of families of circles in the plane. The sequence $(S_n, r_n)_n$ starts with two intersecting circles, (S_0, r_0) and (S_1, r_1), and continues by consistently selecting one intersection point as the centre of the next circle. We set the circle curvatures as $r_n = \frac{1}{a_n}$, for various number sequences $(a_n)_n$ and analyse the positions of the sequence of circle centres. For certain sequences, the respective centres $(S_{2n})_n$ and $(S_{2n+1})_n$ are collinear and converge, and we provide explicit formulas for the coordinates of the limiting centre. This occurs in the case of orthogonal circles. In other cases, the centres of the even- and odd-indexed circles are not collinear. Instead, each subsequent centre is positioned at a specific angle of deflection, and we track the change in the positions of the centres by measuring this angle.

Key words: arrangements of circles, orthogonal circles, limit centre, angle of deflection

MSC 2020: 05B40, 51M04, 52C15

References

[1] Chaplick, S., Förster, H., Kryven, M., Wolff, A., On Arrangements of Orthogonal Circles, *Graph Drawing and Network Visualization: Proceedings of 27th International Symposium, GD 2019*, Prague, Czech Republic, September 17–20, (2019), 216–229.

[2] Došlić, T., Škegro, M., Directed packings of circles in the plane, *Proceedings of the 2nd Croatian Combinatorial Days*, Zagreb, September 27–28, 2018, Eds. Došlić, T., Martinjak, I., (2018), 27–48.

[3] Kang, J. R., Müller, T., Arrangements of Pseudocircles and Circles. *Discrete Comput Geom* **51** (2014), 896–925.

On Translation Curves in $\mathrm{Sol}^4_{m,n}$

Zlatko Erjavec
University of Zagreb Faculty of Organization and Informatics, Varaždin, Croatia
e-mail: zlatko.erjavec@foi.unizg.hr

A translation curve in a Thurston space is a curve such that for given unit vector at the origin, translation of this vector is tangent to the curve in every point of the curve. In most Thurston spaces translation curves coincide with geodesic lines. However, this does not hold for Thurston spaces equipped with twisted product. In these spaces translation curves seem more intuitive and simpler than geodesics.

We present translation curves in 4-dimensional Thurston space $\mathrm{Sol}^4_{m,n}$ and we explore its curvature properties.

Key words: Thurston geometry, $\mathrm{Sol}^4_{m,n}$ space, translation curve

MSC 2020: 53C30, 53C42

References

[1] Belkhelfa, M., Mokni, H., Classification of hypersurfaces in the four dimensional thurston geometry $\mathrm{Sol}^4_{m,n}$, *J. Geom* **116**, 26 (2025).

[2] Erjavec, Z., Geodesics and translation curves in Sol^4_0, *Mathematics* **11** (6) (2023), 1533.

[3] Molnár, E., Szilágyi, B., Translation curves and their spheres in homogeneous geometries, *Publ. Math. Debrecen* **78** (2) (2011), 327–346.

Involute and Evolute of Null Curve in 4-Dimensional Lorentz-Minkowski Space

Ivana Filipan
University of Zagreb Faculty of Mining, Geology and Petroleum Engineering, Zagreb, Croatia
e-mail: ivana.filipan@rgn.hr

Željka Milin Šipuš
University of Zagreb, Faculty of Science, Zagreb, Croatia
e-mail: milin@math.hr

Ljiljana Primorac Gajčić
Josip Juraj Strossmayer University of Osijek, Department of Mathematics, Osijek, Croatia
e-mail: lprimora@mathos.hr

Involutes and evolutes of curves in Euclidean plane were first introduced by Huygens in 1670s, in connection to his work with pendular motion and the isochronous pendulum [1]. The definitions of involutes and evolutes, used in this presentation, are inspired by the analogous definitions for the 4-dimensional Euclidean case [2]. Let $c\colon I \to \mathbb{R}^4_1$ be a (regular) curve in $\mathbb{R}^4_1$.

1. An *involute* $\boldsymbol{i}\colon I \to \mathbb{R}^4_1$ of a curve c is a curve that orthogonally intersects all tangents of the curve c at the corresponding points.
2. An *evolute* $\boldsymbol{e}\colon I \to \mathbb{R}^4_1$ of a curve c is a curve such that c is an involute of $\boldsymbol{e}$.

In the 4-dimensional Lorentz-Minkowski space, the involute and evolute curves of a spacelike curve with non-null normals have been investigated in [6, 7]. Involute and an evolving involute of order k of a null Cartan curve in n-dimensional Minkowski space have been investigated in [3]. In [5] we analyzed involutes of pseudo-null curves in 3-dimensional Lorentz-Minkowski space. Further in [4] we provide a complete classification of involutes and evolutes in the 4-dimensional Lorentz-Minkowski space based on the causal character of the initial curves: Frenet-type, pseudo-null, and partially null curves. We continued our research and investigated properties of involute and evolute of null curve in 4-dimensional Lorentz-Minkowski space and that results are to be presented.

Key words: evolute, involute, null curve, Lorentz-Minkowski space

MSC 2020: 53A10, 53B30

Acknowledgments. This work has been supported by the Next Generation NPOO project (MiNoNePro - Recovery and Resilience Mechanism), funded by the European Union.

References

[1] Boyer, B. C., Merzbach, U. C., *A History of Mathematics*, 3rd ed.; John Wiley & Sons, Inc.: Hoboken, NJ, USA, 2010.

[2] Gerretsen, J. C. H., *Lectures on Tensor Calculus and Differential Geometry*, P. Noordhoff N. V., Groningen, 1962.

[3] Hanifa, M., Hua Houa, Z., Nešović, E., On Involutes of Order k of a Null Cartan Curve in Minkowski Spaces, *Filomat* **33**(8) (2019) 2295–2305.

[4] López, R., Filipan, I., Milin Šipuš, Ž., Primorac Gajčić, Lj., Involutes and evolutes of curves in 4-dimensional Lorentz–Minkowski space, submitted (2026).

[5] López, R., Milin Šipuš, Ž., Primorac Gajčić, Lj., Protrka, I., Involutes of Pseudo-Null Curves in Lorentz–Minkowski 3-Space, *Mathematics* **9**(11) 2021.

[6] Öztürk, G., On Involutes of Order k of a Space-like Curve in Minkowski 4-space $\mathbf{E}_1^4$, *AKU J. Sci. Eng* **16** (2016) 569–575.

[7] Turgut, M., Yilmaz, S., On the Frenet Frame and a Characterization of Space-like Involute-Evolute Curve Couple in Minkowski Space-time, *Int. Math. Forum* **16**(3) (2008) 793–801.

One Geometry, Three Regimes: The Hyperbolic Continuation of Keplerian Conics

Georg Glaeser
University of Applied Arts Vienna, Vienna, Austria
georg.glaeser@uni-ak.ac.at

Previous work revealed a remarkable geometric structure underlying families of elliptic and parabolic Keplerian conics through a fixed point P with common focus F_1. In the present contribution we show that this structure extends naturally beyond escape velocity and gives rise to a corresponding family of hyperbolic flyby trajectories.

Figure 1(a) illustrates the three regimes. For a prescribed velocity direction at P, the elliptic, parabolic, and hyperbolic cases arise as members of a single geometric framework. In all three situations the second focus F_2 lies on the same reflected ray determined by the tangent t at P. In the parabolic limit, F_2 becomes an ideal point.

A particularly simple construction is obtained by prescribing the semimajor axis a; see Figure 1(b). In the elliptic regime one has $PF_2 = 2a - d$, whereas in the hyperbolic regime $PF_2 = 2|a| + d$, where $d = F_1P$. Consequently, the second focus F_2 moves on a circle centered at P. The centers of the conics lie on a second circle, and the family possesses a common envelope. Remarkably, this envelope is an ellipse with foci F_1 and P in both the elliptic and hyperbolic regimes.

We further investigate polar transformations of the flyby family. Polarization with respect to a circle centered at F_1 transforms the hyperbolas into a family of circles, while the common envelope ellipse is transformed into a circle as well. These constructions provide geometric counterparts of the corresponding transformations previously obtained for elliptic and parabolic families.

The results demonstrate that hyperbolic flyby trajectories do not constitute a separate geometric situation. Rather, they arise as the natural continuation of the full family of Keplerian conics and share the same underlying geometric structure.

Key words: Keplerian conics, flyby hyperbolas, envelope ellipse, vis-viva equation, polar transformation

MSC 2020: 70F15, 51A05, 51N20, 37J35

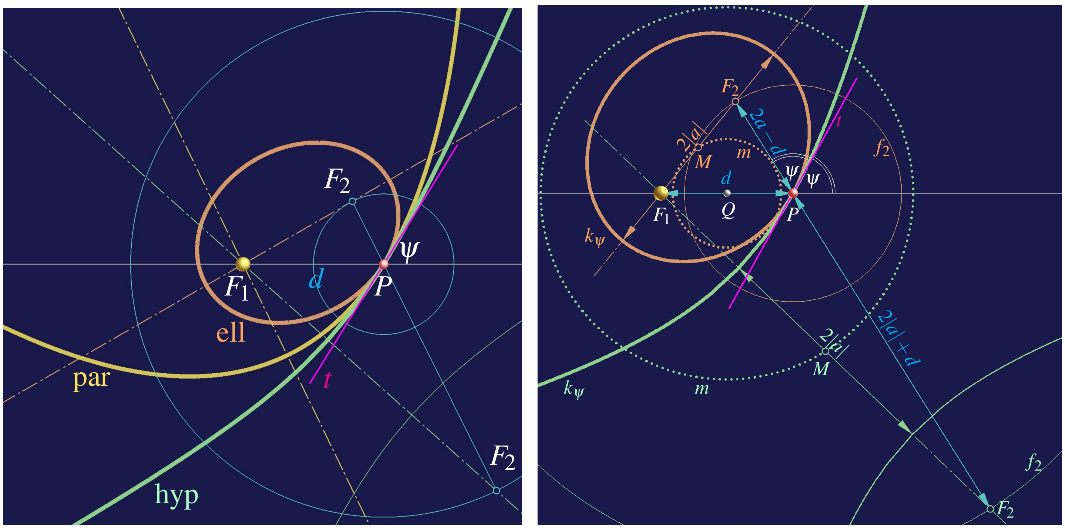

(a) Three regimes of Keplerian conics through P.

(b) Unified construction for prescribed semimajor axis a.

Figure 1: (a) Elliptic, parabolic, and hyperbolic Keplerian conics through the fixed point P with common focus F_1. In all three cases the second focus F_2 lies on the same reflected ray; in the parabolic limit it becomes an ideal point.
(b) Construction of the family for prescribed semimajor axis a. In the elliptic regime $PF_2 = 2a - d$, whereas in the hyperbolic regime $PF_2 = 2|a| + d$. Consequently, the second focus moves on a circle centered at P.

References

[1] Glaeser, G., From Keplerian Ellipse Families to the Set of Keplerian Parabolas, *Proceedings of the 22nd International Conference on Geometry and Graphics* (ICGG 2026), Vol. 1, Springer, Cham, 2026.

[2] Glaeser, G., Geometric Construction of a Family of Keplerian Ellipses, *KoG* **29** (2025), 53–62, `https://doi.org/10.31896/k.29.6`

[3] Glaeser, G., One Geometry, Three Regimes: The Hyperbolic Continuation of Keplerian Conics, *KoG* **30** (2026), to appear.

Smooth Ride - Bicycle Track Design by Free-form Curves

Miklós Hoffmann
Eszterházy Károly Catholic University, Eger, Hungary
e-mail: hoffmann.miklos@uni-eszterhazy.hu

Ede Troll
Eszterházy Károly Catholic University, Eger, Hungary
e-mail: troll.ede@uni-eszterhazy.hu

Two closely related scenarios of bicycle wheel track design by free-form curves are investigated. In the first, the track of the bicycle front wheel is prescribed and the rear wheel track is computed. For a rational Bézier front wheel track we write the "bicycle equation" as a Riccati equation with rational coefficients. We describe a solution that produces rear wheel tracks as piecewise rational Bézier/NURBS curves with guaranteed error bounds. We also show that for Pythagorean-hodograph curve as front wheel track, several expressions are further simplified.

In the second, complementary viewpoint the rear wheel track is prescribed and the front wheel track is to be computed. It is proved that if the rear wheel track is given as a PH curve, then the front wheel track can be described as an exact rational Bézier/NURBS representation. It is also proved that the PH condition is genuinely special in this regard: for any other standard polynomial, rational or even trigonometric spline curve type as rear wheel track, the associated front wheel track cannot be represented exactly as a standard CAD curve.

Key words: bicycle track design, PH curve, NURBS representation

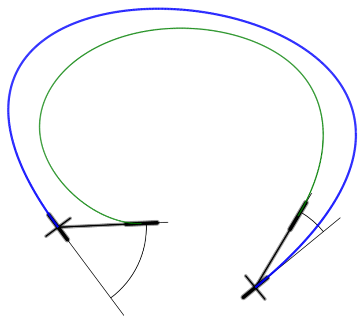

Figure 1

References

[1] Farouki, R. T, *Pythagorean-hodograph curves: algebra and geometry inseparable*, Springer, 2008

[2] Levi, M., Tabachnikov, S., On bicycle tire tracks geometry, hatchet planimeter, Menzin's conjecture, and oscillation of unicycle tracks, *Exp. Math.* **18** (2009), 173–186.

Near-Equilateral Recurrence of Rotating Points

Iva Kodrnja
University of Zagreb Faculty of Geodesy, Zagreb, Croatia
e-mail: iva.kodrnja@geof.unizg.hr

Mia Maras
University of Zagreb Faculty of Geodesy, Zagreb, Croatia
e-mail: mmaras@geof.hr

Let O be the origin point. Three points P_i, $i = 1, 2, 3$ rotating around O at the same distance with angular velocities ω_i have periods of rotation $T_i = 2\pi/\omega_i$ and angular displacement $\theta(t) = t\omega_i + \omega_{i_0}$, with ω_{i_0} being the initial position of point P_i.

Consider the three hands of a clock as three points rotating on a circle, Fig. 1. An ideal analog clock has periods $T_h = 720$, $T_m = 60$ and $T_s = 1$ in minutes and is an example of a periodical system, the whole configuration returning to the initial position every 12 hours. To understand the periodicity and recurrence we consider two functions measuring relative angular displacement for two pairs of points $\theta_{i1}(t) = (\omega_i - \omega_1)t, i = 2, 3$. The question we are interested in is whether the points ever reach an equilateral configuration, $\theta_{21}(t) = \pm 120°$, $\theta_{31}(t) = \pm 240° (\mod 360°)$, and if they don't what is the recurrence time of a near-equilateral configuration given a predefined threshold $\varepsilon > 0$. There is no exact solution for a regular triangle formed by ideal clock hands.

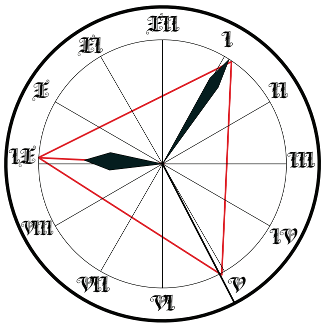

Figute 1: Three hands of a clock in a near-equilateral formation

In Fig. 2 we see two Lissajous curves relating frequencies found in the clock; a) relative motion of an ideal hour and minute hands, $\omega_1 = 1$ and $\omega_2 = 1/12$, where the 11 double points represent the 11 recurrences of particular arrangement (displacement) of the two hands in one orbital period, the most famous being their conjunction (in Croatian there is a saying *When the hands of a clock coincide, it means someone is thinking about you.*) and in part b) we see the relation of two angular displacements for the hour hand, $\theta_{21}(t)$ and $\theta_{31}(t)$, having the same number of double points, but this curves is showing quasiperiodic behaviour, it never closes.

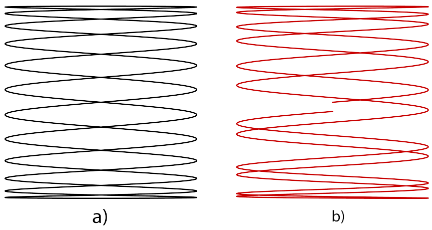

Figure 2: Lissajous curves $\{\sin(\omega_1 t), \sin(\omega_2 t)\}$ for $t \in [0, 12\mathrm{h}]$

Orbital resonance problems naturally arise in the study of planetary dynamics [1], as well in kinematics, [2]. In this talk we are interested in simplified problems concerning planar uniform rotation and principles of periodicity and quasiperiodicity of near-equilateral formations for a finite number of points uniformly rotating around a fixed point. We will also look at 'geocentric' calculations, for instance we look at four points rotating around $\mathcal{O}$ and search for near-equilateral conditions for three points on epitrochoid curves around the fourth point, as if we are looking at regular triangular arrangements of three planets in the night sky, Figure 3.

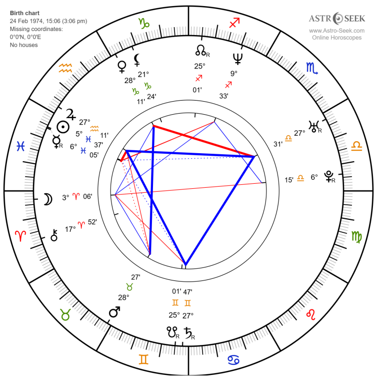

Figure 3: In 1974 Jupiter, Saturn and Uranus were in near-equilateral figuration around Earth, [3].

Key words: uniform rotation, polygon, orbital period, epitrochoids

MSC 2020: 53A04, 37E15

References

[1] Caritá, G. A., Signor, A. C., Morais, M. H. M., A numerical study of the 1/2, 2/1 and 1/1 retrograde mean motion resonances in planetary systems, *Monthly Notices of the Royal Astronomical Society* **515**(2) (2022), 2280–2291.

[2] Rochera, D., Curves that allow the motion of a regular polygon, *Aequat. Math.* **99** (2025), 377–395.

[3] AstroSeek, `https://www.astro-seek.com/`, accessed 2.7.2026.

Geometry for All: Removing Barriers for Students with Disabilities

Darija Marković
University of Osijek, Faculty of Civil Engineering and Architecture, Osijek, Croatia
e-mail: dmarkovic1@gfos.hr

Josipa Matotek
University of Osijek, Faculty of Civil Engineering and Architecture, Osijek, Croatia
e-mail: matotek@gfos.hr

The increasing number of students with disabilities and learning difficulties at all levels of education calls for a reconsideration of how geometry is taught and experienced. Although inclusive education has become an important priority in contemporary educational systems, geometry remains one of the most demanding areas of mathematics due to its strong dependence on visual-spatial reasoning, abstract thinking, language comprehension, and complex problem-solving processes.

Students with diverse learning needs often face significant barriers when learning geometry, which may negatively affect their participation, confidence, and academic achievement. At the same time, teachers and higher education instructors are increasingly challenged to provide learning environments that accommodate a wide range of abilities, backgrounds, and learning profiles.

This presentation will discuss current trends related to the growing diversity of learners and examine the specific challenges associated with geometry education from primary school to higher education. It will highlight the importance of accessible learning environments, flexible teaching practices, and the potential of emerging digital technologies to support equitable participation and improve learning outcomes.

The presentation aims to encourage discussion on how geometry education can evolve to become more accessible, engaging, and inclusive, ensuring that all learners have the opportunity to develop geometric thinking and participate fully in the learning process.

Key words: students with disabilities, higher education, geometry learning, learning barriers, digital technologies

MSC 2020: 97Gxx, 97C30, 97C70

Bézier Curves are not Smooth!

Boris Odehnal
University of Applied Arts, Department of Geometry, Vienna, Austria
e-mail: boris.odehnal uni-ak.ac.at

Bézier curves allow for polynomial or rational parametrizations which make them parts of algebraic curves of genus 0. As such, a Bézier curve of degree d carries the maximal number of simple singularities – or the delta invariants of all its singularities sum up to $\frac{1}{2}(d-1)(d-2)$ – that can occur on an algebraic curves of degree d. While the singularities on cubic Bézier curves are simple ones (either a node or a cusp), the singularities on curves of degree $d \geq 4$ can be *compound singularities*, *i.e.*, they can be limits of certain numbers of infinitely close ordinary singularities.

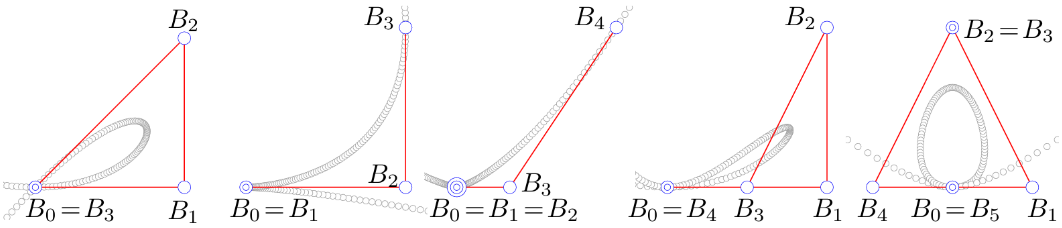

Figute 1: Five control polygons for Bézier curves that exhibit various singularities: (i) an ordinary node and (ii) a cusp on cubic Bézier curves, (iii) a cusp of the third kind on a quartic Bézier curve, (iv) a tacnode on a quartic Bézier curve, and (v) an osculation node on a quintic Bézier curve.

In the interrior of the unit interval $[0, 1]$ over which Bézier curves are defined they are smooth. However, they lack global smoothness and an algebraic curve has to exhibit singularities in order to be rational (of genus 0).

We shall demonstrate that an occasionally improper choice of the configuration of control points can result in singularities of arbitrary complexity and curves with any possible type of singularity can be modeled with a Bézier curve (cf. Fig. 2). The presence of the polynomial (or rational) parametrization of genus zero curves in the vicinity of singularities immediately yields local expansions in terms of power series (not only formal power series like the Puiseux series).

We shall stroll through the garden of singularities, thereby not necessarily aiming at a complete collection of possible combinations of singularities on Bézier curves of degree up to 5. There is indeed a variety of 122 different types Bézier curves of degree 5 if we only count all possible combinations of different types of singularities on rational quintic Bézier curves, not distinguishing between real or complex images. Some examples are shown in Fig.. 3.

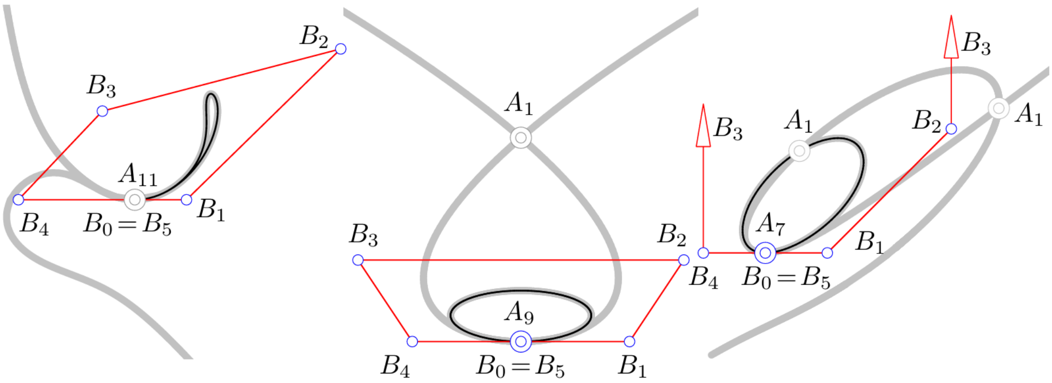

Figute 2: Properly and improperly chosen control points lead to Bézier curves with singularities in any case: An A_{11} or $[2, 6, 2]$ singularity (left), an A_9 or $[2, 5, 2]$ together with an ordinary node A_1 or $[2, 1, 2]$ (middle), and an A_7 or $[2, 4, 2]$ singularity with two A_1 singularities occur on (rational) quintic Bézier curves with the given control polygon.

From the viewpoint of Descriptive Geometry (in higher dimensional spaces), the singularities can be created by applying a specific projection of a rational normal curve onto the projective plane. This approach also clarifies why and which types of singularities may occur on Bézier curves.

Key words: Bézier curve, compound singularity, parametrization, control structure

MSC 2020: 14H20, 14H50, 51N05

Axial Extremal Configurations for Bicentric Pentagons

Mandi Orlić Bachler
Zagreb University of Applied Sciences, Zagreb, Croatia
e-mail: mandi.orlic@tvz.hr

We study the extrema of the area in a one-parameter Poncelet family of bicentric pentagons. Let C_2 be the circumcircle with centre O and radius R, and let C_1 be the incircle with centre I, radius r, and centre distance $d = OI$. The parameters are assumed to satisfy the Fuss relation for a bicentric pentagon, so Poncelet's porism gives a family of pentagons inscribed in C_2 and tangent to C_1. Using the half-angle parametrization of C_2, the problem is reduced to a one-variable area function $J_B(t_1)$ on a fixed convex branch B.

Two axial configurations play the central role. In one of them a vertex lies at $(R, 0)$, and in the other a vertex lies at $(-R, 0)$. We denote the corresponding area values by P_R and P_L.

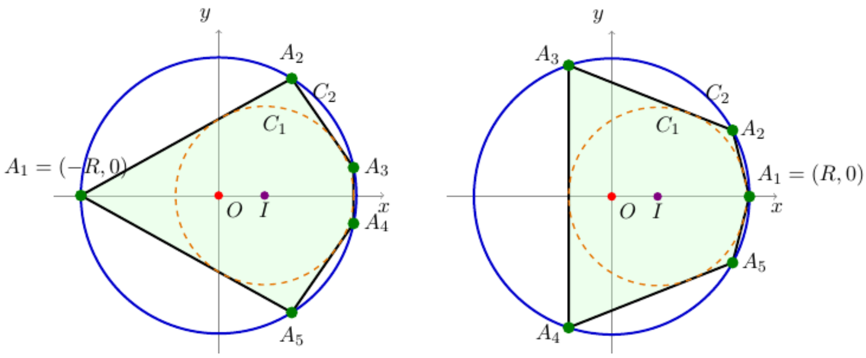

Figure 1: The two axial configurations for the numerical example $R = 1$ and $d = \frac{1}{3}$. Left: the configuration with area value P_L. Right: the configuration with area value P_R.

For these two configurations one obtains the explicit formulas

$$P_R = r\left(\frac{3R+d}{R-d}\sqrt{(R-d)^2 - r^2} + 2\sqrt{R^2 - (d-r)^2}\right),$$

and

$$P_L = r\left(\frac{3R-d}{R+d}\sqrt{(R+d)^2 - r^2} + 2\sqrt{R^2 - (d+r)^2}\right).$$

The main result is that, on the chosen non-degenerate convex branch,

$$P_R < P_L,$$

and that these two axial levels exhaust the extremal values. Hence the minimum of the area is attained on the axial orbit containing the vertex $(R, 0)$, while the maximum is attained on the axial orbit containing the vertex $(-R, 0)$.

The proof combines a reflection argument, symbolic elimination, and an elliptic-curve interpretation of the complex Poncelet correspondence. Reflection shows that every axial-vertex configuration is stationary, while elimination gives the corresponding projective axial factor. To exclude non-axial critical points, the oriented area is lifted to a meromorphic function $\mathcal{J}$ on the elliptic normalization E of the tangency correspondence. A local calculation gives

$$\deg \operatorname{Pole}(d\mathcal{J}) \leq 20.$$

The reflection-reversal involutions show that the pull-back of the axial divisor is contained in the zero divisor of $d\mathcal{J}$; this pull-back also has degree 20. Therefore all zeros of $d\mathcal{J}$ are axial, and no non-axial critical points occur on the chosen convex branch.

This gives a complete description of the extremal area behaviour for the selected bicentric Poncelet family of pentagons and illustrates how classical Poncelet geometry can be combined with explicit algebraic and elliptic-curve methods.

Key words: bicentric polygon, Poncelet porism, area, Fuss relation, pentagon

MSC 2020: 51M16, 51M25, 51N20

Acknowledgments. This work was supported by the Croatian Science Foundation project HRZZ-IP-2024-05-3882.

References

[1] Gulasekharam, F. H. V., Poncelet's Poristic Polygons, *Math. Gaz.* **25** (1941), no. 263, 28–35.

[2] Josefsson, M., Minimal area of a bicentric quadrilateral, *Math. Gaz.* **99** (2015), no. 545, 237–242. `https://doi.org/10.1017/mag.2015.32`

[3] Josefsson, M., Maximal area of a bicentric quadrilateral, *Forum Geom.* **12** (2012), 237–241.

[4] Orlić Bachler, M., Kaliman, Z., O površini bicentričnog četverokuta, *AMSD* **6** (2023), Art. 7. `https://doi.org/10.32817/amssd.6.7`

[5] Radić, M., Certain inequalities concerning bicentric quadrilaterals, hexagons and octagons, *Journal of Inequalities in Pure and Applied Mathematics* **6** (2005), Art. 1.

Computable Closedness of Incidence Relations in Effective Topological Geometry

Bojan Pažek
Faculty of Electrical Engineering, Computer Science and Information Technology
Josip Juraj Strossmayer University of Osijek, Osijek, Croatia
e-mail: bpazek@ferit.hr

Classical incidence geometry studies relations such as point-line incidence, collinearity and concurrence. We ask when such closed incidence relations are effectively available, in the sense that both positive and negative finite information can be obtained from a given effective basis. The background comes from computable topology and computable analysis, where closed sets are studied through c.e. closedness, co-c.e. closedness and computable closedness [2, 1, 9, 8]. Related results show that topological assumptions can turn semicomputable or co-c.e. information into computability [6, 7, 5]. We apply this viewpoint to topological incidence structures whose spaces and incidence relations carry computable finite-information data.

Let $\mathbf{X} = (X, \mathcal{T}_X, (I_i)_{i\in\mathbb{N}})$ and $\mathbf{L} = (L, \mathcal{T}_L, (J_j)_{j\in\mathbb{N}})$ be computable topological spaces, interpreted as the spaces of points and lines. A computable incidence space is a triple

$$\mathfrak{X} = (\mathbf{X}, \mathbf{L}, \mathrm{On}),$$

where $\mathrm{On} \subseteq X \times L$ is the primitive point-line incidence relation, assumed computable closed in the product computable topological space $\mathbf{X} \times \mathbf{L}$. For $n \geq 2$, define

$$\mathrm{Inc}_n = \{(x_1, \dots, x_n, \ell) \in X^n \times L : (x_k, \ell) \in \mathrm{On} \text{ for all } k\},$$

and

$$\mathrm{Col}_n = \{(x_1, \dots, x_n) \in X^n : \exists \ell \in L,\ (x_1, \dots, x_n, \ell) \in \mathrm{Inc}_n\}.$$

Thus

$$\mathrm{Col}_n = \pi_{X^n}(\mathrm{Inc}_n).$$

The difficulty is that collinearity is obtained by projection, i.e. by an existential quantifier over the line space.

Main theorem. *Let $\mathbf{Y}$ be a computable topological space and let $\mathbf{L}$ be an effectively compact computable topological space. If $A \subseteq Y \times L$ is computable closed in $\mathbf{Y} \times \mathbf{L}$, then $\pi_Y(A) \subseteq Y$ is computable closed in $\mathbf{Y}$.*

The proof is an effective version of the tube lemma: the positive information is preserved by product neighborhoods, while effective compactness of $\mathbf{L}$ makes the negative part of the projection effective.

It follows from this theorem that if $\mathrm{Inc}_n \subseteq X^n \times L$ is computable closed in $\mathbf{X}^n \times \mathbf{L}$, and if $\mathbf{L}$ is effectively compact, then the derived collinearity relation

$$\mathrm{Col}_n \subseteq X^n$$

is computable closed in $\mathbf{X}^n$. Hence all finite collinearity relations are computable closed whenever the corresponding finite incidence relations are computable closed and the line space is effectively compact.

In the real projective plane, one may take $X = \mathbb{RP}^2$ and $L = (\mathbb{RP}^2)^*$. The point-line incidence relation is

$$\mathcal{I} = \{(x, \ell) \in X \times L : x \in \ell\},$$

and

$$\mathrm{Col}_3 = \pi_{X^3}\{(x_1, x_2, x_3, \ell) : x_1, x_2, x_3 \in \ell\}.$$

Thus the theorem gives a finite-information criterion for effective collinearity. For example, classical incidence theorems, such as Menelaus' theorem and Ceva's theorem, give explicit coordinate descriptions of such conditions [3]. Thus computable closed incidence relations provide positive and negative certificates for geometric constraints, a viewpoint related to certified geometric computation [4] and potentially useful for future geometry-aware machine learning.

Key words: computable topological space, incidence geometry, computable closed sets, collinearity, projective geometry, effective compactness, Menelaus' theorem

MSC 2010: 03D78, 51A05, 51H10, 54D30

Acknowledgments. This research was funded by the European Union – NextGenerationEU through the project DigSTEM-UP, funding number 581-UNIOS-39.

References

[1] Brattka, V., Presser, G., Computability on subsets of metric spaces, *Theoret. Comput. Sci.* **305**(1–3) (2003), 43–76, `https://doi.org/10.1016/S0304-3975(02)00693-X`.

[2] Brattka, V., Weihrauch, K., Computability on subsets of Euclidean space I: closed and compact subsets, *Theoret. Comput. Sci.* **219**(1–2) (1999), 65–93, `https://doi.org/10.1016/S0304-3975(98)00284-9`.

[3] Coxeter, H.S.M., Greitzer, S.L., *Geometry Revisited*, Mathematical Association of America, Washington, D.C., 1967.

[4] Edalat, A., Khanban, A. A., Lieutier, A., Computability in computational geometry, in: S. B. Cooper, B. Löwe and L. Torenvliet (eds.), *New Computational Paradigms*, CiE 2005, Lect. Notes Comput. Sci. **3526**, Springer, Berlin, Heidelberg, 2005, 117–127, `https://doi.org/10.1007/11494645\_15`.

[5] Horvat, M., Iljazović, Z. Pažek, B., Computability of pseudo-cubes, *Ann. Pure Appl. Logic* **171**(8) (2020), 102823.

[6] Iljazović, Z., Co-c.e. spheres and cells in computable metric spaces, *Log. Methods Comput. Sci.* **7**(3:05) (2011), 1–21, `https://doi.org/10.2168/LMCS-7(3:05)2011`.

[7] Iljazović, Z., Pažek, B., Co-c.e. sets with disconnected complements, *Theory Comput. Syst.* **62**(5) (2018), 1109–1124.

[8] Vuković, M., *Izračunljivost*, skripta, Sveučilište u Zagrebu, 2009.

[9] Weihrauch, K., Grubba, T., Elementary computable topology, *J. Univers. Comput. Sci.* **15**(6) (2009), 1381–1422.

Ruled Surfaces of Cube Gears

Lukas Rose
University of Applied Arts, Department of Geometry, Vienna, Austria
lukas.rose@uni-ak.ac.at

Boris Odehnal
University of Applied Arts, Department of Geometry, Vienna, Austria
boris.odehnal@uni-ak.ac.at

We choose a tetrahedron within a cube and rotate the corresponding vertex stars. Those vertex stars rotate with the same speed about the space diagonals of the cube. We investigate the orbits of intersection lines of neighbouring faces. In order to describe these surfaces analytically, we employ Rodrigues' rotation formula to obtain explicit parametrizations of the rotating edges and faces. Via Weierstrass substitution, we convert the trigonometric parametrizations into rational forms, enabling a determination of implicit equations. Thus, we obtain the equations of ruled surfaces swept by certain edges in the course of the motion. These ruled surfaces are algebraic and of degree three and four. The double curve of the quartic ruled surface consists of an ellipse and an intersecting straight line. The cubic and the quartic ruled surfaces are contained in hyperbolic linear line congruences. We further examine algebraic and geometric properties of these surfaces, *i.e.*, their behavior at infinity, their double curves. The results illustrate how rotational symmetries of a polyhedral framework give rise to intricate algebraic surfaces. In particular, we show that for a certain instant of the rotation, the rotating edges together with the intersection lines of adjacent faces is congruent to the edge-skeleton of a deltoidal dodecahedron.

Key words: cube kinematic, ruled surfaces

MSC 2020: 14J26, 70B10

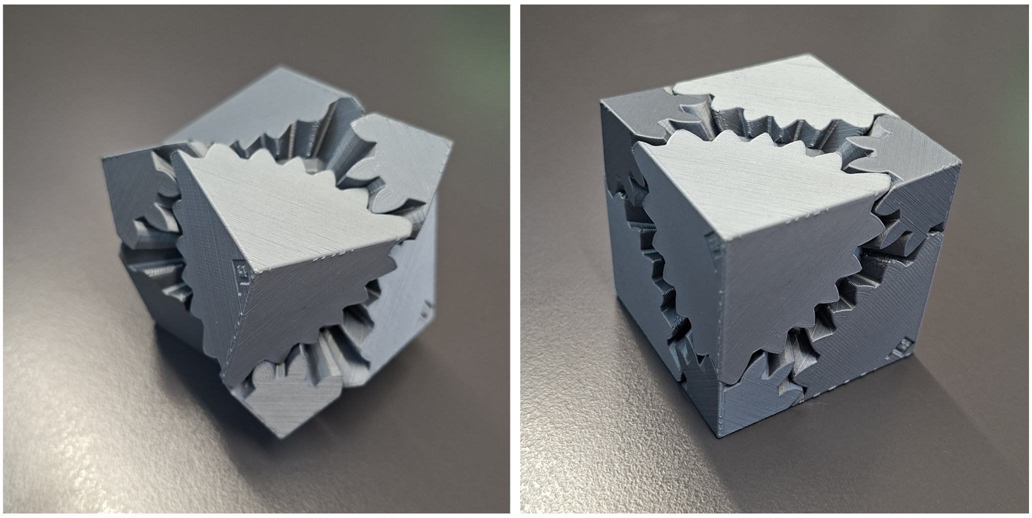

Figure 1: 3d printed cube gears

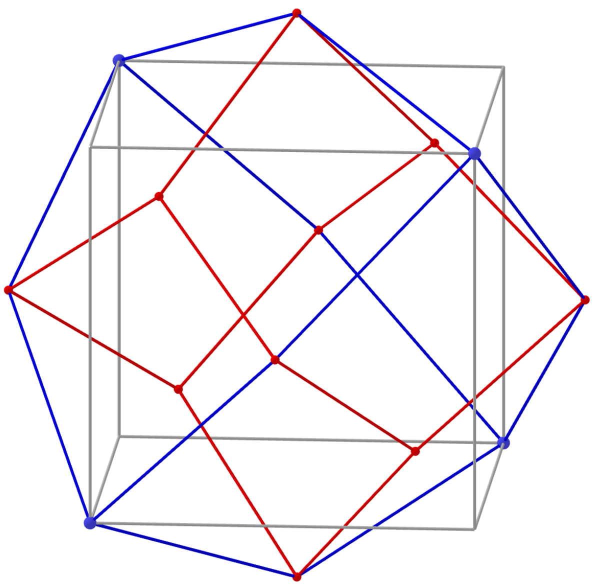

Figure 2: Deltoidal dodecahedron, with the vertices and edges of the rotated starting cube in blue and the intersection points and lines of the rotated faces in red

Lattice-like Packings and Coverings with Congruent Translation Balls and Cylinders in Sol Geometry

Judit Sajtos
Budapest University of Technology and Economics, Budapest, Hungary
e-mail: sajt.judith@gmail.com

Jenő Szirmai
Budapest University of Technology and Economics, Budapest, Hungary
e-mail: szirmai@math.bme.hu

The eight Thurston geometries are one of the more significant areas of modern mathematics and the question of sphere coverings and sphere packings has a special importance in crystallography, since atoms can be modeled with spheres. Thus these questions represent important research directions in all eight mentioned geometries.

The classification of the lattices of the **Sol** space was done in the work [2]; an important type among these are the so-called fundamental lattices. The investigation of translation sphere packings belonging to them was done in the work [4], which we aimed to continue and extend in our work, [3].

We investigated the lattice-like coverings of the **Sol** space connected to its fundamental lattices both with congruent translation spheres and with a new type of cylinder of the **Sol** space, also defined by us. To do this, among other things, we studied the convexity of the translation spheres in the Euclidean sense, in order to guarantee the covering. We proved that a translation sphere in the **Sol** space is convex in the Euclidean sense if its radius $r \leq \frac{\pi}{2}$.

We introduced the covering density of each covering and gave an upper bound to them using the radius and volume of the sphere circumscribing a given *translation tetrahedron*, as well as the volume of the cylinder.

We also examined the same type of cylinder packings and their density for fundamental lattices and even gave a general upper bound density of cylinder packings without any symmetry assumption.

In our work, we use the unified projective model of Thurston geometries (see [1], [5]) to visualize the **Sol** geometry and to calculations.

Key words: Thurston geometries, **Sol** geometry, translation-like bisector surface of two points, circumscribed sphere of **Sol** tetrahedron and its convexity, Dirichlet-Voronoi cell

MSC 2020: 53A20, 52C17, 53A35, 52C35, 53B20

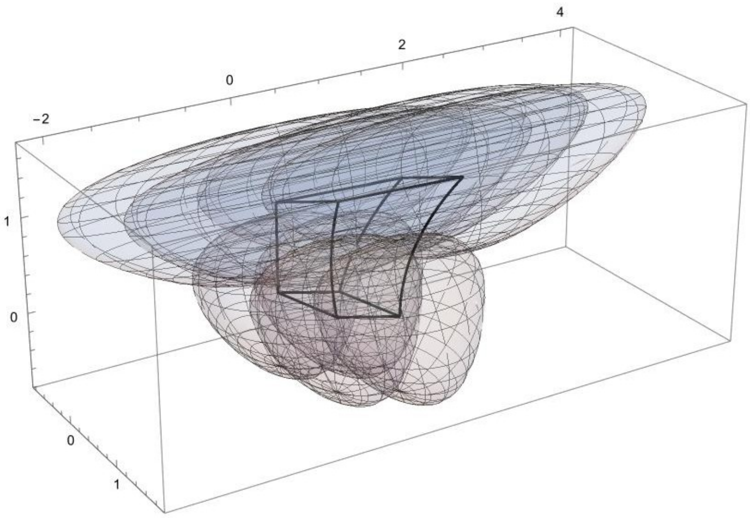

Figure 1: Locally optimal lattice-like translation ball covering of a fundamental lattice with density $\Delta_\Gamma^C \approx 6.47048$.

References

[1] Molnár, E., The projective interpretation of the eight 3-dimensional homogeneous geometries, *Beitr. Algebra Geom.* **38**(2) (1997), 261–288.

[2] Molnár, E., Szirmai, J., Classification of **Sol** lattices, *Geom. Dedicata* **161**(1) (2012), 251–275.

[3] Sajtos, J., Szirmai, J., Lattice-like packings and coverings with congruent translation balls and cylinders in Sol geometry, *Quaest. Math.* (2026), 1–23. `https://doi.org/10.2989/16073606.2026.2649569`

[4] Szirmai, J., The densest translation ball packing by fundamental lattices in **Sol** space, *Beitr. Algebra Geom.* **51**(2) (2010), 353–373.

[5] Szirmai, J., Bisector surfaces and circumscribed spheres of tetrahedra derived by translation curves in **Sol** geometry, *New York J. Math.* **25** (2019), 107–122.

On Congruent Tetrahedra with Crossing Edges

Hellmuth Stachel
Vienna University of Technology, Vienna, Austria
e-mail: stachel@dmg.tuwien.ac.at

Two congruent regular tetrahedra $\mathcal{T}_1$ and $\mathcal{T}_2$ forming a Stella Octangula allow a continuous motion of $\mathcal{T}_2$ relative to $\mathcal{T}_1$ such that each edge of $\mathcal{T}_2$ slides along an edge of $\mathcal{T}_1$. Recently, E. Makai and T. Tarnai [1] and G. Weiss proved that the same property holds for congruent tetrahedra $\mathcal{T}_1$, $\mathcal{T}_2$ of much more general shape. In [2] one- and even two-parametric relative motions of this type were disclosed. In each position, there exists a reflection in a point, line or plane that sends $\mathcal{T}_1$ to $\mathcal{T}_2$. It remained open whether these are the only possible relative motions $\mathcal{T}_2/\mathcal{T}_1$ of congruent tetrahedra (note [1], Problem 1). The goal of this lecture is to close this gap.

Key words: tetrahedron, Stella Octangula, Euclidean motion

MSC 2020: 51N20, 52C25

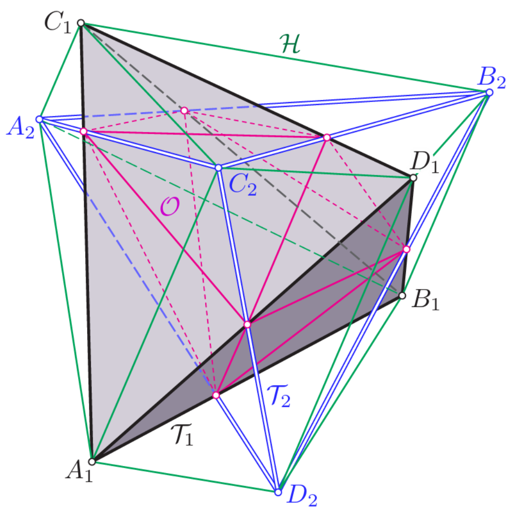

Figure 1: Two congruent regular tetrahedra $\mathcal{T}_1$, $\mathcal{T}_2$ with crossing edges, i.e., with six edge-contacts. The intersection of the solids is a convex octahedron $\mathcal{O}$, their convex hull is the cuboid $\mathcal{H}$, i.e., a hexahedron with six quadrangular faces.

References

[1] Makai, E., Tarnai, T., Generalized Forms of an Overconstrained Sliding Mechanism Consisting of Two Congruent Tetrahedra, *Stud. Sci. Math. Hung.* **60**(1) (2023), 43–75.

[2] Stachel, H., Weiss, G., Stellae Octangulae in Motion Revisited, *KoG* **29** (2025), 3–17.

Thinking First, Prompting Second – A Complex AI System for Problem-Solving Support

Ede Troll
Eszterházy Károly Catholic University, Eger, Hungary
e-mail: troll.ede@uni-eszterhazy.hu

One of the most pressing tasks facing education and educational institutions is to develop a pedagogically grounded response to the growing presence of artificial intelligence, to integrate it into teaching and learning in a meaningful and beneficial way, and to address the risks arising from its uncontrolled or merely execution-oriented use. A central challenge in the educational use of general-purpose language models is that AI frequently functions as a direct executor. Rather than fostering meaningful dialogue or eliciting student reasoning, it often generates complete solutions without additional clarification. Such output cannot, by itself, be regarded as the student's own independent problem-solving outcome and does not facilitate the development of solution strategies, the identification of subproblems, or the understanding of domain-specific decisions. Over-reliance on AI-generated solutions may reduce students' active cognitive engagement and adversely affect critical thinking, analytical reasoning, and independent decision-making [5, 1]. Additionally, generated responses may not correspond to the student's prior knowledge, course requirements, or the pedagogical objectives of the task [3]. As a result, mathematically or technically correct solutions may still be unnecessarily complex from an educational standpoint, difficult to interpret, or reliant on concepts not yet introduced.

To address these challenges, this work presents the development and current prototype of a multi-component AI system designed to provide structured guidance throughout the problem-solving process rather than supplanting student effort. Related approaches use knowledge tracing and turn-by-turn verification to guide students through coding tasks [2], as well as pedagogy-guided agents that determine when and how instructional feedback should be provided [4]. Our system comprises two closely integrated AI components with distinct functions. One component executes individual subtasks, including calculations, technical implementations, and the generation of intermediate results. The other manages communication with the student, interprets and refines requests, and guides the problem-solving process through targeted questions and feedback. It forwards well-specified subtasks to the execution-oriented component and directs its operation.

Within this framework, three principal actors interact: the instructor, the student, and the AI system. The instructor defines the task, specifies the permitted knowledge space, and identifies the subject-specific aspects and subproblems that the student is expected to address. The student interprets and decomposes the problem, formulates explicit instructions for the AI, and evaluates, verifies, and, when necessary, modifies the results. The AI system assesses student prompts in terms of completeness, clarity, alignment with the defined knowledge space, and coverage of the required aspects, thereby supporting subsequent stages of the problem-solving process.

The presentation introduces the system's architecture, operational logic, and pedagogical foundations. Although the system is not discipline-specific, the discussion concludes with examples from secondary-school geometry to illustrate how its current version supports task structuring, guides student reasoning, and generates partial solutions aligned with the intended level of mathematical knowledge.

Key words: AI-assisted learning, problem solving, mathematics education, geometry education

MSC 2020: 97D50, 97U50, 68T50

References

[1] Bauer, E., Greiff, S., Graesser, A. C., Scheiter, K., Sailer, M., Looking beyond the hype: Understanding the effects of AI on learning, *Educ. Psychol. Rev.* **37** (2025), Art. 45.

[2] Wang, J., Dai, Y., Zhang, Y., Ma, Z., Li, W., Chai, J., Training turn-by-turn verifiers for dialogue tutoring agents: The curious case of LLMs as your coding tutors, in *Findings of the Association for Computational Linguistics: ACL 2025*, Association for Computational Linguistics, 2025, 12416–12436.

[3] Yan, L., Sha, L., Zhao, L., Li, Y., Martínez-Maldonado, R., Chen, G., Li, X., Jin, Y., Gašević, D., Practical and ethical challenges of large language models in education: A systematic scoping review, *Br. J. Educ. Technol.* **55** (2024), 90–112.

[4] Yang, Q., Yang, Y., An, S., Hao, T., Xu, G., LLM-based collaborative agents with pedagogy-guided interaction modeling for timely instructive feedback generation in task-oriented group discussions, in *Proceedings of the Thirty-Fourth International Joint Conference on Artificial Intelligence*, International Joint Conferences on Artificial Intelligence, 2025, 9972–9980.

[5] Zhai, C., Wibowo, S., Li, L. D., The effects of over-reliance on AI dialogue systems on students' cognitive abilities: A systematic review, *Smart Learn. Environ.* **11** (2024), Art. 28.

Conoids in 4D

Daniela Velichová
Slovak University of Technology in Bratislava, Bratislava, Slovakia
e-mail: daniela.velichova@stuba.sk

Conoids are amazig surfaces forming quite considerable part of classical geometric studies with relevant practical applications. Wonderfull synthetic constructions have been discovered for manual drawings of various types of conoids, based on geometric relations of these non-developable ruled surfaces. One of the most fascinating examples of this surface family are, with no doubts, Plűcker and Kűpper conoids. Line constructions of these surfaces are hopefully still well-known and taught at the faculties of architecture and civil engineering. In mathematics, these two surfaces are recognized as parts of graphs of special rational functions with two variables.

Although almost everything had been already discovered about conoids, there exist another and unexpected definitions of these surfaces. Conoids might be generated as products of Minkowski point set operations of line segments and circles positioned to different planes in 4-dimensional space. We will present these constructions and illustrate 3D images of generated 4D conoids in double orthogonal projection and 4D perspective. Particular case of a special conoid generated in this way is illustrated in the Figure 1.

Key words: conoids, Minkowski operations in 4D

MSC 2020: 51N05, 51N25, 65D17

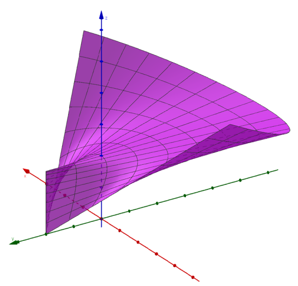

Figure 1: Conoid from 4D

References

[1] Hamilton, W. R., *Lectures on Quaternions*, Hodges & Smith, Dublin, 1853.

[2] Velichová, D., Minkowski Operations in Modeling Manifolds, *IMACS Series in Computational and Applied Mathematics*, **Vol. 20**, Roma 2017, 171–180.

[3] Zamboj, M., Double orthogonal projection of four-dimensional objects onto two perpendicular three-dimensional spaces, *Nexus Netw. J.*, **20**(1) (2018), 267–281.

Three Points and their Place of Action – Still a Matter of Attraction

Gunter Weiss
Dresden University of Technology, Dresden, Germany
Vienna University of Technology, Vienna, Austria
e-mail: weissgunter@gmx.net

To three points in a Euclidean plane there exist thousands of "triangle centers" and curves collected in C. Kimberling's famous "Encyclopedia of Triangle Centers". Obviously, many of the constructions of such triangle centers can be modified for classical Cayley-Klein geometries, too. Here we start with a more general viewpoint: We consider three basic elements in ring geometries, focusing on Möbius and Laguerre Geometry and their model spaces. Similarly, one can start with three skew lines of the real 3-dimensional projective space and map them to three points of the so-called Klein quadric in a projective 5-space. Three Euclidean motions also will occur as three points on the hyperquadric model of the set of motions. In all these cases, the geodesics connecting pairs of points in the model spaces are straight lines, such that one in fact deals with a classical triangle/trilateral in the model spaces. Finally, the triangle centers and objects connected with the triangle in the model space should be interpreted in the original set of objects.

Key words: triangle geometry, Möbius geometry, Laguerre geometry, projective space

MSC 2020: 51M05, 51C05

References

[1] Benz, W., *Vorlesungen über Geometrie der Algebren*, Springer-Verlag, 2012.

[2] Kimberling, C., *Encyclopedia of Triangle Centers*, `https://faculty.evansville.edu/ck6/encyclopedia/etc.html` (last access January 2026).

Practical Considerations for Optimal Transport based Shape Morphing in Blender

Leonard Weydemann
University of Applied Arts Vienna, Department of Geometry, Vienna, Austria
e-mail: leonard.weydemann@uni-ak.ac.at

We present a Blender add-on that integrates optimal transport (OT) methods for 3D Shape interpolation. Building on prior research, we implement an optimal transport solution within the Blender Python scripting environment. Particular consideration is given to the practicability of this approach to real life problems.
As demonstrated in prior work, OT is effective for interpolating between 3D shapes by creating a Wasserstein barycenter between two point clouds. Our implementation leverages this ability to handle meshes with differing vertex counts to perform interpolation-driven repair and morphing. Implemented within Blender's scripting environment we present a production-ready plugin and evaluate practical concerns, such as: computational cost and execution time, parameter tuning and usability, compatibility with existing Blender pipelines (e.g., remeshing and retexturing), and texture reprojection.
We validate the approach through a set of real-world case studies, assessing performance, integration quality, and the add-on's utility for common mesh-processing workflows.

Key words: Optimal Transport, Wasserstein barycenter, Blender, computational geometry, Python scripting, customizable software, Open Source Software

MSC 2020: 68U05, 97P40, 68U07

Figure 1: This figure shows the Wasserstein barycenter of the Max Planck and Nefertiti scan (center). The result is triangulated via the Ball pivot algorithm. For scan sources please refer to: [2].

References

[1] Blender Online Community, Blender – a 3D modeling and rendering package, Stichting Blender Foundation, Amsterdam, `http://www.blender.org`.

[2] Common 3d test models, `https://github.com/alecjacobson/common-3d-test-models`

[3] Solomon, J., de Goes, F., Peyré, G., Cuturi, M., Butscher, A., Nguyen, A., Du, T., Guibas, L., Convolutional wasserstein distances: efficient optimal transportation on geometric domains, *ACM Trans. Graph.* **34**(4) (2015), Art. 66.

[4] Delon, J., Gozlan, N., Saint Dizier, A., Generalized Wasserstein barycenters between probability measures living on different subspaces *Ann. Appl. Probab.* **33**(6A) (2023), 4395–4423.

[5] Cuturi, M., Doucet, A., Fast computation of Wasserstein barycenters *International conference on machine learning* (2014), 685–693.

[6] Bonneel, N., Digne, J., A survey of optimal transport for computer graphics and computer vision *Comput. Graph. Forum* **42**(2) (2023), 439–460.

Posters

Geometric Bliss Beyond the Circle Kiss

Maja Andrić
University of Split, Faculty of Civil Engineering, Architecture and Geodesy, Split, Croatia
e-mail: maja.andric@gradst.hr

Dominka Jukić
University of Split, Faculty of Civil Engineering, Architecture and Geodesy, Split, Croatia
e-mail: dominka.jukic@gradst.hr

Neda Lovričević
University of Split, Faculty of Civil Engineering, Architecture and Geodesy, Split, Croatia
e-mail: neda.lovricevic@gradst.hr

Reading the poem *The Kiss Precise* by the English Nobel laureate Frederick Soddy, we notice an unusual intertwining of mathematical concepts and poetry. And indeed, hidden within the poem is an entire theorem about a trio of mutually tangent circles (or "kissing circles"), which is itself connected to the famous problem posed by the ancient Greek "great geometer" Apollonius of Perga:

"To construct all circles in a plane that are tangent to three given circles."

By carefully reading the stanzas of Soddy's poem, we decipher their true meaning.

Key words: circle, Apollonius' problem

MSC 2020: 51M04

References

[1] Palman, D., *Geometrijske konstrukcije*, Element, 1996.

[2] Palman, D., *Trokut i kružnica*, Element, 2024.

Take it, Invert it, Solve it and Bring it Back

Gorana Aras-Gazić
University of Zagreb Faculty of Architecture, Zagreb, Croatia
e-mail: gorana.aras-gazic@arhitekt.unizg.hr

Ana Laštre
University of Split, Faculty of Science, Split, Croatia
e-mail: alastre@pmfst.hr

Many challenging geometric problems become surprisingly simple when viewed through the lens of inversion: take the figure, invert it, solve the easier problem, and bring the solution back to the original setting. This poster introduces the method of inversion, its fundamental properties, and its advantages in geometry. We discuss several classical results in which inversion plays a central role, including the theorems of Miquel, Ptolemy and Feuerbach. Finally, we present the analytical formulation of inversion in Cartesian coordinates and illustrate how it can be used to transform and solve geometric problems. From an educational perspective, inversion is highly valuable in high school mathematics competitions, where it enables elegant solutions to difficult problems, and at the university level, where it strengthens geometric intuition and links classical geometry with modern analytic approaches.

Key words: inversion, circle, line

MSC 2020: 97G10, 97G50

References

[1] Palman, D., *Geometrijske konstrukcije*, Element, 1996.

[2] Palman, D., *Trokut i kružnica*, Element, 2004.

[3] Šiljak, H., *Inverzija*, math.e, Vol.14, 2009.

Algebraic Surfaces in Civil Engineering and Architecture

Ivana Božić Dragun
University of Applied Sciences, Zagreb, Croatia
e-mail: ivana.bozic@tvz.hr

Antonela Orkić
University of Applied Sciences, Zagreb, Croatia
e-mail: antonela.orkic@tvz.hr

Algebraic surfaces are fundamental geometric objects defined as the zero sets of polynomial equations in three variables. Their geometric properties, including order, class, and degree, provide a mathematical framework for describing and analysing complex three-dimensional forms. Among these surfaces, ruled quadrics are of particular interest because they combine rich geometric structure with practical applicability.

This poster presents the basic classification of algebraic surfaces and highlights the role of ruled surfaces in civil engineering and architecture [1]. Through selected examples, including hyperboloids, hyperbolic paraboloids, and conical surfaces, it demonstrates how geometric properties influence structural behaviour and enable the design of efficient lightweight structures. The transition from classical geometric constructions to modern computational and parametric design illustrates the continuing importance of algebraic geometry in contemporary engineering.

Key words: algebaraic surfaces

MSC 2020: 97G80, 97G99

Figure 1

References

[1] Božić Dragun, I., Orkić, A., Algebraic Surfaces In Civil Engineering And Architecture, *Polytechnic and Design*, in press (2026)

Geometric Characterisation of Recycled Crushed Brick Aggregate in Sustainable Concrete

Marijana Hadzima-Nyarko
Josip Juraj Strossmayer University of Osijek, Faculty of Civil Engineering and Architecture, Osijek, Croatia
e-mail: mhadzima@gfos.hr

Silva Lozančić
Josip Juraj Strossmayer University of Osijek, Faculty of Civil Engineering and Architecture, Osijek, Croatia
e-mail: lozancic@gfos.hr

Antonija Ereš
Josip Juraj Strossmayer University of Osijek, Faculty of Civil Engineering and Architecture, Osijek, Croatia
e-mail: aeres@gfos.hr

Josip Radić
Josip Juraj Strossmayer University of Osijek, Faculty of Civil Engineering and Architecture, Osijek, Croatia
e-mail: jradic@gfos.hr

Daniela Đikanović
University of Belgrade, Institute for Multidisciplinary Research, Belgrade, Serbia
e-mail: djikanovic.daniela@gmail.com

The development of sustainable building materials with recycled components requires an interdisciplinary approach that combines materials engineering with geometric analysis of material structure. Within the IM4STEM project, concrete is being investigated to reduce construction waste and create more sustainable materials. Particular attention is given to aggregate, a key constituent of concrete that significantly influences its strength, stiffness, and mechanical behaviour under loading. As aggregates constitute the largest volume fraction of concrete, their geometry and macroscopic composition directly affect the material's properties.

This paper analyses the geometric characteristics of recycled crushed brick aggregate, including particle shape, size distribution, porosity, and spatial relationships within the cement matrix. Aggregate geometry influences the compactness of the concrete mixture, interfacial bonding, and stress distribution, while its macroscopic composition affects the material's mechanical performance and durability. The microstructure of the composites is further examined using microscopy, enabling a more detailed analysis of pore distribution, the interaction between the cement matrix and recycled aggregate, and the influence of particle geometry on the material structure. Microscopic imaging also provides quantitative information on pore morphology and the spatial distribution of aggregate particles, supporting the geometric characterisation of the composite at the microscale.

The research shows that a properly selected granulometric composition and a reduced proportion of poorly shaped particles can significantly improve the properties of cement composites containing recycled materials. The study highlights the crucial role of geometric concepts in understanding and optimising sustainable composites, and demonstrates the benefits of interdisciplinary integration between geometry, materials science, and modern STEM fields.

Key words: recycled crushed brick aggregate, sustainable concrete, geometric characterisation, granulometric composition, microstructure

Inversion on the Cyclic Quadrangle in the Isotropic Plane

Ema Jurkin
University of Zagreb Faculty of Mining, Geology and Petroleum Engineering, Zagreb, Croatia
e-mail: ema.jurkin@rgn.unizg.hr

Marija Šimić Horvath
University of Zagreb Faculty of Architecture, Zagreb, Croatia
e-mail: marija.simic@arhitekt.unizg.hr

In this talk, we present additional properties of the geometry of the cyclic quadrangle in the isotropic plane. The focus of our study is on its diagonal quadrangle and its nine-point conic. We prove that the nine-point conic of the quadrangle is a special hyperbola with the center in the centroid of the quadrangle. Next, we define the inversion with respect to the circumcircle of the quadrangle and the absolute point as the pole. It is shown that the nine-point conic of the quadrangle is mapped onto a 3-circular cubic, and that the Euler circle of the diagonal triangle is the inverse image of the circumcircle of the diagonal triangle. Moreover, we obtain the following result: a unique cubic passing through the vertices of the quadrangle is invariant under defined inversion. It is 2-circular cubic and passes through the vertices of the diagonal triangle and its pedal triangle as well.

Key words: isotropic plane, cyclic quadrangle, diagonal triangle, inversion

MSC 2020: 51N25

Acknowledgments. This work has been supported by the Next Generation NPOO project (MiNoNePro - Recovery and Resilience Mechanism), funded by the European Union.

References

[1] Jurkin, E., Automorphic Inversion and Circular Quartics in Isotropic Plane, *KoG* **12** (2008), 19–26.

[2] Schmidt, E., Der Mittenkegelschnitt eines Sehnenvierecks, `http://eckartschmidt.de/Mitkg.pdf`

[3] Schmidt, E., Rund um den Polar-Kreis, `http://eckartschmidt.de/Polar.pdf`

[4] Volenec, V., Beban-Brkić, J., Šimić, M., The cyclic quadrangle in the isotropic plane, *Sarajevo J. Math.* **7** (2011), 265–275.

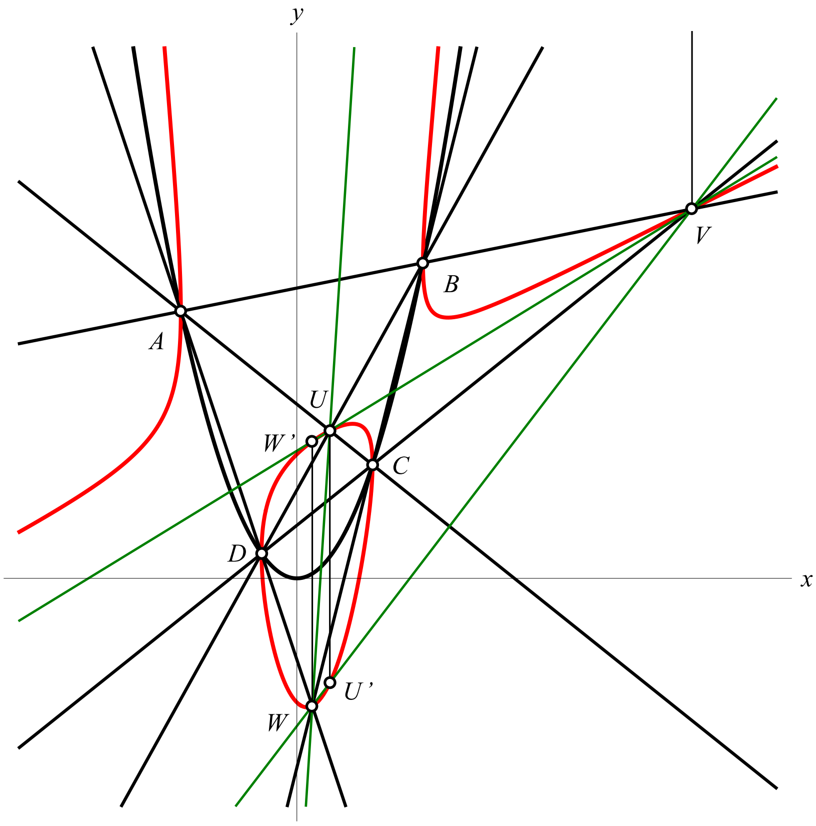

Figure 1: Cyclic quadrangle with its diagonal triangle and cubic curve invariant under defined inversion

List of participants

1. Davor Andrić
   University of Zagreb Faculty of Architecture
   davor.andric@arhitekt.unizg.hr
2. Maja Andrić
   University of Split, Faculty of Civil Engineering, Architecture and Geodesy
   maja.andric@gradst.hr
3. Gorana Aras-Gazić
   University of Zagreb Faculty of Architecture
   garas@arhitekt.hr
4. Tamás Balla
   Eszterházy Károly Catholic University, Eger
   balla.tamas@uni-eszterhazy.hu
5. Ivana Božić Dragun
   Zagreb University of Applied Sciences
   ivana.bozic@tvz.hr
6. Christian Clemenz
   University of Applied Arts Vienna
   christian.clemenz@uni-ak.ac.at
7. Géza Csima
   Budapest University of Technology and Economics, Institute of Mathematics
   csgeza@math.bme.hu
8. Petra Daković
   University of Zagreb Faculty of Organization and Informatics
   pdakovic@foi.hr
9. Blaženka Divjak
   University of Zagreb Faculty of Organization and Informatics
   blazenka.divjak@foi.unizg.hr
10. Zlatko Erjavec
    University of Zagreb Faculty of Organization and Informatics
    zlatko.erjavec@foi.unizg.hr

11. Ivana Filipin
University of Zagreb Faculty of Mining, Geology and Petroleum Engineering
ivana.filipan@rgn.unizg.hr

12. Georg Glaeser
University of Applied Arts Vienna, Department of Geometry
georg.glaeser@uni-ak.ac.at

13. Marijana Hadzima-Nyarko
University of Osijek, Faculty of Civil Engineering and Architecture
jmhadzima@gfos.hr

14. Miklos Hoffmann
Eszterházy Károly Catholic University, Eger
hoffmann.miklos@uni-eszterhazy.hu

15. Ema Jurkin
University of Zagreb Faculty of Mining, Geology and Petroleum Engineering
ema.jurkin@rgn.unizg.hr

16. Iva Kodrnja
University of Zagreb Faculty of Geodesy
ikodrnja@geof.hr

17. Biserka Kolarec
University of Zagreb Faculty of Agriculture
bkudelic@agr.hr

18. Helena Koncul
University of Zagreb Faculty of Civil Engineering
helena.koncul@grad.unizg.hr

19. Nikolina Kovačević
University of Zagreb Faculty of Mining, Geology and Petroleum Engineering
nikolina.kovacevic@rgn.hrr

20. Ana Laštre
University of Split, Faculty of Science
alastre@pmfst.hr

21. Neda Lovričević
University of Split, Faculty of Civil Engineering, Architecture and Geodesy
neda.lovricevic@gradst.hr

22. Darija Marković
University of Osijek, Faculty of Civil Engineering and Architecture
dmarkovic1@gfos.hr

23. Josipa Matotek
University of Osijek, Faculty of Civil Engineering and Architecture
josipa.matotek@gfos.hr

24. Damir Mikoč
University of Zadar, Department of Teacher Education Studies in Gospić
damir.mikoc@gmail.com

25. Željka Milin Šipuš
University of Zagreb Faculty of Science
milin@math.hr

26. Boris Odehnal
University of Applied Arts Vienna
boris.odehnal@uni-ak.ac.at

27. Mandi Orlić Bachler
University of Applied Sciences Zagreb
mandi.orlic@tzv.hr

28. Bojan Pažek
Rudolfovo Science and Technology Center, Novo mesto
bojan.pazek@rudolfovo.eu

29. Ljiljana Primorac Gajčić
University of Osijek, Department of Mathematics
ljiljana.primorac@mathos.hr

30. Lukas Rose
University of Applied Arts Vienna
Lukas.Rose@uni-ak.ac.at

31. Judit Sajtos
Budapest University of Technology and Economics
sajtjudith@gmail.com

32. Hellmuth Stachel
Vienna University of Technology
stachel@dmg.tuwien.ac.at

33. Jenő Szirmai
Budapest University of Technology and Economics
szirmai@math.bme.hu

34. Marija Šimić Horvath
University of Zagreb Faculty of Architecture
marija.simic@arhitekt.unizg.hr

35. David Tarandek
Faculty of Architecture, University of Zagreb
dtarandek@arhitekt.hr

36. Ede Mátyás Troll
Eszterházy Károly Catholic University, Eger
troll.ede@uni-eszterhazy.hu

37. Daniela Velichová
Slovak University of Technology in Bratislava
daniela.velichova@stuba.sk

38. Gunter Weiss
Vienna University of Technology, Dresden University of Technology
weissgunter@gmx.net

39. Leonard Weydemann
University of Applied Arts Vienna
leonard.weydemann@uni-ak.ac.at

40. Michal Zamboj
Charles University, Prague
michal.zamboj@pedf.cuni.cz